JOURNAL OF CATALYSIS 75, 337–353 (1982)

Uncatalyzed and Platinum-Catalyzed Gasification of Carbon by Water and Carbon Dioxide

W. L. HOLSTEIN AND M. BOUDART[1]

Department of Chemical Engineering, Stanford University, Stanford, California 94305

Received October 30, 1981; revised January 13, 1982

Differential rates and integral surface time yields of the uncatalyzed and platinum-catalyzed gasification of carbon by H_2O and CO_2 were measured above and below 950 K, respectively, at pressures below amospheric. Both the uncatalyzed and catalyzed reactions were inhibited by their products. At 890 K the catalyzed reactions were about 100 times faster than the uncatalyzed reactions. Reaction orders of the platinum-catalyzed gasification of carbon by H_2O with respect to H_2O and H_2 and kinetic isotope effects in H_2O/H_2 and D_2O/D_2 suggest equilibration between gaseous H_2O and H_2 (or D_2O and D_2) and surface atomic oxygen. The latter yields CO by reaction with carbon which has been transported to the platinum surface following breakage of carbon–carbon bonds at the platinum–carbon interface. The selectivity of carbon gasification to CO, CO_2, and CH_4 indicates that CO_2 is produced from CO by water–gas shift, while CH_4 is produced by hydrogenolysis of carbon. The platinum-catalyzed gasification of carbon by CO_2 proceeds through a similar series of steps as that for the gasification by H_2O.

INTRODUCTION

Several reviews have been written on the uncatalyzed (*1, 2*) and catalyzed (*3–5*) gasification of carbon by water and carbon dioxide. The primary reaction between H_2O and carbon is

$$\text{(I)}\quad C + H_2O = CO + H_2.$$

In addition, there are two secondary gas–gas reactions, water–gas shift and methanation,

$$\text{(II)}\quad CO + H_2O = CO_2 + H_2,$$

$$\text{(III)}\quad CO + 3H_2 = CH_4 + H_2O.$$

Finally, H_2 and CO_2 produced in reactions (I)–(III) can react directly with the carbon in the hydrogenolysis and carbon dioxide gasification reactions respectively:

$$\text{(IV)}\quad C + 2H_2 = CH_4,$$

$$\text{(V)}\quad C + CO_2 = 2CO.$$

Analysis of reaction (I) is complicated by the numerous secondary reactions which may occur, only two of which are linearly independent. The reaction between carbon dioxide and carbon is somewhat easier to study since it involves only reaction (V).

Unlike reaction (IV) studied earlier (*6*), reactions (I) and (V) are not limited by equilibrium at pressures below atmospheric and high temperatures.

Uncatalyzed Gasification of Carbon by Water and Carbon Dioxide

The following rate equations have been proposed for the $C–H_2O$ reaction:

$$r = \frac{\alpha(H_2O)}{1 + \beta(H_2) + \gamma(H_2O)} \quad (7–9), \quad (1)$$

$$r = \frac{\alpha(H_2O)}{1 + \beta(H_2)^{1/2} + \gamma(H_2O)} \quad (10), \quad (2)$$

$$r = \alpha[H_2O)/(H_2O)]^n \quad (11), \quad (3)$$

where $0 < n < 1$, and at low hydrogen pressures only:

$$r = \frac{\alpha(H_2)}{[1 + \beta(H_2O)^{1/2}]^2} \quad (12). \quad (4)$$

Some results are reported only in terms of the apparent reaction order in H_2O:

$$r = \alpha(H_2O)^n \quad (13, 14). \quad (5)$$

[1] To whom inquiries should be sent.

0021-9517/82/060337-17$02.00/0

Similarly, rate equations for the $C-CO_2$ reaction are

$$r = \frac{\alpha(CO_2)}{1 + \beta(CO) + \gamma(CO_2)} \quad (8, 15\text{–}17), \tag{6}$$

$$r = \alpha(CO_2)^n \quad (13). \tag{7}$$

The $C-H_2O$ and $C-CO_2$ reactions are both inhibited by products. The reactions may be studied differentially using H_2O-H_2 and CO_2-CO feed streams or by integrating an assumed rate equation through the bed. The latter approach has been taken in most studies. Discrimination among Eqs. (1)–(3) for the $C-H_2O$ reaction is difficult because of secondary reactions involved, internal mass transfer effects at high rates, and possible changes in the rate as the carbon surface changes during gasification. Kinetic analysis at high conversion of reactant (*18*) is very complicated.

The most likely values of the activation energies of the $C-H_2O$ and $C-CO_2$ reactions when the inhibitor term is dominant in the denominator of Eqs. (1) and (6) are 335 and 360 kJ mol^{-1}, respectively. The rate equations and the activation energies for the two reactions are similar. In addition the rates are nearly the same, the rate of gasification by H_2O being a factor of 3 greater at 1073 K and a reactant pressure of 10 kPa. These factors suggest a similar mechanism for both reactions (*1*).

The two gasification reactions have been proposed (*1*) to occur through the following steps, the first one being equilibrated and the second rate determining:

$$\ldots C-C-C^* + RO \rightleftharpoons \ldots C-C-CO + R,$$

$$\ldots C-C-CO \rightarrow \ldots C-C^* + CO,$$

where

$R \equiv H_2$ for the $C-H_2O$ reaction,

$R \equiv CO$ for the $C-CO_2$ reaction.

The carbon–carbon bond is broken in the rate-determining second step. Product inhibition results from equilibration of the first step. Equations (1) and (6) result from this mechanism for a uniform surface. Equation (3) results from a nonuniform surface (*19*). Most recent work supports this mechanism (*2*).

Catalyzed Gasification of Carbon by Water and Carbon Dioxide

The effect of catalysts on the rates of carbon gasification have been studied in several investigations and reviewed recently (*3–5*). While many studies have reported the relative activities and activation energies of a series of catalysts for the gasification of carbon by CO_2 (*20–22*) or H_2O (*22–26*), very little work has been devoted to obtaining reaction orders.

Several mechanisms have been proposed to explain the accelerated rates of carbon gasification in the presence of a catalyst. These are summarized below.

The electron transfer mechanism (*27*) states that the catalyst serves to either donate or accept π electrons to or from the carbon, resulting in a weakening in the strength of the carbon–carbon bonds on the edge planes of the carbon. These carbon atoms, at the active sites on the carbon away from the catalyst, are more readily gasified to carbon monoxide by carbon dioxide or water due to this weakening in the carbon–carbon bond strength.

The oxygen transfer mechanism (*3, 5*) states that the catalyst goes through an oxidation–reduction cycle, resulting in the oxidation of carbon to carbon monoxide at the catalyst–carbon interface. The iron-catalyzed $C-CO_2$ reaction (*5, 28*) has been proposed to occur through the two-step mechanism:

$$\begin{aligned} CO_2 + Fe^* &= Fe^*-O + CO \\ Fe^*-O + C &= Fe^* + CO \\ \hline CO_2 + C &= 2CO \end{aligned}$$

The alkali metal-catalyzed $C-H_2O$ reaction (*29*) has been proposed to occur through

the following series of reactions:

$$M_2CO_3 + 2C = 2M + 3CO$$
$$2M + 2H_2O = 2MOH + H_2$$
$$\underline{2MOH + CO = M_2CO_3 + H_2}$$
$$2C + 2H_2O = 2CO + 2H_2$$

Similar series of steps have been proposed for the alkali metal-catalyzed $C-CO_2$ reaction (*30*) and the alkaline earth metal-catalyzed $C-H_2O$ reaction (*31*).

Intercalation of the catalyst into the carbon has also been proposed. An intercalated metal atom could serve to act as an electron donor and accelerate the rate in a way similar to that proposed in the electron transfer mechanism (*32*) or through an oxidation–reduction cycle involving formation of the intercalation complex as the reduced state of the catalyst (*4*).

Two factors must be considered in analyzing the results of the catalytic oxidation of carbon by H_2O and CO_2: the chemical state of the catalyst and pore diffusion effects.

The chemical state of the catalyst has been found to have a profound effect on gasification rates. For example, while iron is a very active catalyst for the gasification of carbon by carbon dioxide, wüstite (FeO) is less active and magnetite (Fe_3O_4) is totally inactive (*5, 31*). A decrease in the rate of the gasification of carbon by carbon dioxide catalyzed by nickel and iron with time has been noted due to the conversion of the metals to nickel oxide (NiO) and wüstite, respectively (*33*).

The chemical state of the catalyst is particularly difficult to determine for alkali metal catalysts, which may be present as the base metal, the oxide, or the carbonate during the gasification of carbon by carbon dioxide. In addition, the hydroxide may be present during the gasification of carbon by water.

The influence of pore diffusion on the kinetics of gas–carbon reactions has been discussed extensively (*1*). Special care must be taken in defining the conditions for which internal diffusion effects mask the true kinetics for reactions which are inhibited by products (*34*). Otto and Shelef (*25*) have taken pore diffusion into account in analyzing the gasification of carbon by water for several catalysts. Most other catalytic investigations, however, have neglected pore diffusion problems.

Platinum-Catalyzed Gasification of Carbon by Water and Carbon Dioxide

The Pt-catalyzed $C-H_2O$ (*22, 24, 25*) and $C-CO_2$ (*22, 35*) reactions have been studied (Tables 1 and 2).

The addition of 0.8 to 5% platinum to carbon is reported to accelerate its rate of gasification by H_2O and CO_2 by a factor of 10 to 100 (*22, 24, 25, 35*). Reaction orders have not been reported for either reaction. The activation energy for the Pt-catalyzed $C-H_2O$ reaction is reported to be 250 kJ mol^{-1} by Otto and Shelef (*25*) and calculated to be 175 ± 15 kJ mol^{-1} from the data of Rewick *et al.* (*24*), while that for the Pt-catalyzed $C-CO_2$ reaction has not been reported. The products of the Pt-catalyzed $C-H_2O$ reaction have been reported to be solely CO and H_2 (*24*) and CO, CO_2, and H_2 (*22*). No rate equations have been reported for either reaction and there is no accepted mechanism.

The kinetics of the reactions and the product selectivity of the $C-H_2O$ reaction were studied to gain insight into the role of platinum.

EXPERIMENTAL

Spheron 6, a high-purity (99.95%) channel black made by the Godfrey Cabot Corporation was selected because of its purity and high specific surface area. It consists of almost spherical nonporous particles 15 nm in radius. The preparation of 1% Pt/Spheron samples referred to as Pt/C has been described elsewhere (*36*).

Hydrogen and deuterium (99.95%) were purified by diffusion through palladium. He-

TABLE 1

Previous Kinetic Studies of the Pt-Catalyzed C–H_2O Reaction

Reference	Catalyst	Method	$\frac{r_{cat}}{r_{uncat}}$ [a]	x [b]	n [c]	E (kJ mol^{-1}) [d]	Products
22	4.8% Pt/C [f]	Flow-through, gravimetric and gas analysis	≳6	*e*	*e*	*e*	CO, CO_2, H_2
24	0.8% Pt/C [g]	Recirculating, gravimetric	10	*e*	*e*	175	CO, H_2
25	1% Pt/C [h]	Flow-through, gas analysis	30	*e*	*e*	250	*e*

[a] Relative rate of catalyzed to uncatalyzed reaction.
[b] Space velocity dependence (rate $\sim S^x$).
[c] Reported reaction order.
[d] Reported activation energy.
[e] Not determined.
[f] Active carbon, Shirasagi C (Takeda Chemical Industry).
[g] Sterling FT, a channel black (Cabot).
[h] SP-1 Graphite (Union Carbide).

TABLE 2

Previous Kinetic Studies of the Pt-Catalyzed $C-CO_2$ Reaction

Reference	Catalyst	Method	$\frac{r_{cat}}{r_{uncat}}$[a]	x[b]	n[c]	E (kJ mol^{-1})[d]
22	4.8% Pt/C[f]	Flow-through, gravimetric and gas analysis	≥6	*e*	*e*	*e*
35	5% Pt/C[g]	Flow-through, gas analysis	≥40	*e*	*e*	*e*

[a] Relative rate of catalyzed to uncatalyzed reaction.
[b] Space velocity dependence (rate $\sim S^x$).
[c] Reported reaction order.
[d] Reported activation energy.
[e] Not determined.
[f] Active carbon, Shirasagi C (Takeda Chemical Industry).
[g] Active carbon, origin not reported.

lium (99.995%) and carbon dioxide (99.9%) were used as received. Distilled water and deuterated water (99.84%) from Bio-Rad Laboratories were purged of dissolved gases by bubbling helium through the water at room temperature until no impurities were measured by gas chromatography. The bubbling was then continued for an additional 2 h.

The experimental system is shown in Fig. 1. In all runs, the same weight (5 g) of carbon or Pt/C was charged into a quartz-fixed bed reactor contained in a high-temperature furnace (*37*). The sample was pretreated at 1225 K in flowing helium at atmospheric pressure for 2 h to remove adsorbed surface oxides present on the carbon and provide a reproducible state for kinetic measurements.

Data for the $C-H_2O$ reaction were obtained by bubbling He or H_2–He mixtures through a two-stage saturator maintained at a known temperature from 273 to 323 K in a water bath. Data for the $C-D_2O$ reactions were obtained similarly with a second saturator containing D_2O. Vapor pressure data for H_2O (*38*) or D_2O (*39*) were used to determine the partial pressure of H_2O or D_2O in the gas stream at atmosphere pressure leaving the saturators. The total flow rate of gas leaving the saturator was regulated to be 11.1 liters (STP) h^{-1} at all times, except when altered to determine the influence of space velocity on the reaction. Lines carry-

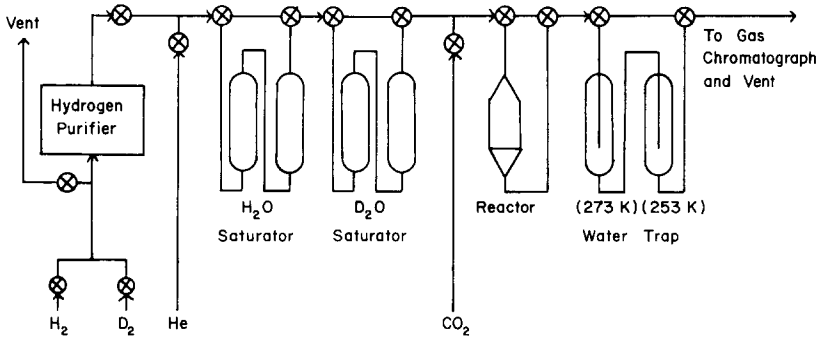

FIG. 1. Experimental apparatus.

ing the gas stream from the saturator to the reactor were jacketed with heating tape to ensure that no water condensation occurred. Water was condensed from the gas stream exiting the reactor by a two-stage condensor, the first stage in an ice bath and the second stage in an ethylene glycol/water slush bath at about 253 K.

Products (CO, CO_2, and CH_4) were analyzed in a gas chromatograph equipped with a thermal conductivity detector. Products were separated by a Poropak Q Column, maintained at either 303 or 323 K. The higher temperature allowed for higher sensitivity but resulted in incomplete separation of H_2 and CO peaks at high H_2 and low CO concentrations. For this case the lower temperature was used. The gas chromatograph was calibrated by means of calibrating gas mixtures obtained from Matheson. Concentrations of H_2 were determined by mass balance.

Data for the $C-CO_2$ reaction were obtained by flowing CO_2–He mixtures at atmospheric pressure through the packed bed of carbon or Pt/C and measuring the exit concentration of CO.

For the $C-H_2O$ reaction, the conversion of H_2O was kept below 10% at all times and was generally less than 4%. With H_2O-H_2–He feed mixtures the concentration of H_2 increased through the bed by less than 20% and generally less than 10%. For the $C-CO_2$ reaction the conversion of CO_2 was below 5% and generally less than 2%.

The kinetic isotope effect was measured as follows. An H_2O-H_2–He feed mixture was flowed through the packed bed of carbon, and the production of CO, CO_2, and CH_4 were measured. The H_2 flow was stopped, and the H_2O saturator was bypassed by the He. Helium purged the reactor, and D_2 purged the hydrogen purifier for 5 min. A D_2–He feed mixture was then saturated with D_2O and flowed through the reactor. The D_2 flow rate was controlled to be the same as the previous H_2 flow rate. The temperature of the D_2O saturator was adjusted to ensure that the partial pressure of D_2O in the gas leaving the saturator was the same as the previous partial pressure of H_2O. After a period of at least 15 min, the production of CO, CO_2, and CD_4 by the D_2O-D_2–He feed mixture was measured. The rates of reaction for H_2O-H_2–He were the same before and after the D_2O-D_2–He measurements were made, within experimental error.

The relative rate of gasification in H_2O–He and CO_2–He mixtures was measured by the following procedure. An H_2O–He feed mixture was flowed through the packed bed of carbon and the production of CO and CO_2 were measured. The system was purged with He for 5 min. A CO_2–He feed mixture with a CO_2 partial pressure equal to the previous H_2O partial pressure was then flowed through the packed bed of carbon, and after a period of at least 30 min the production of CO was measured. The procedure was reversed and the production of CO and CO_2 by H_2O–He was again measured. The rates of reaction in H_2O–He before and after the CO_2–He were identical, within experimental error.

RESULTS

The initial BET surface area was 102 m^2 g^{-1} for the carbon and 91 m^2 g^{-1} for the Pt/C. After pretreatment of the latter, the dispersion of the platinum was 48% by hydrogen titration of preadsorbed oxygen (*40*). There was no need to measure the changing surface area of the carbon or the changing dispersion of the platinum during the course of the reaction because rates were very low and only small changes occurred during the course of the measurements. All rates represent mass (ng) of carbon gasified per second and per unit initial surface area (m^2) of carbon. The symbol r is used for differential rates where the rate is constant through the carbon bed. The symbol r' is used for surface time yields, where the rate changes through the bed due to product inhibition. For the catalyzed $C-H_2O$ reaction, where the carbon is gasified to CO, CO_2, and CH_4,

TABLE 3

Summary of Kinetic Results for the Uncatalyzed C–H_2O and C–CO_2 Reactions

Feed	T (K)[a]	P(kPa)[b]		x[c]	n[d]		E (kJ mol^{-1})[e]	r (ng m^{-2} s^{-1})[f]
		H_2O, CO_2	H_2		H_2O, CO_2	H_2		
H_2O	940–1070	0.8–12.3	—	0.32 ± 0.05	0.54 ± 0.05	—	230 ± 20	9.0[g]
H_2O–H_2	980–1100	0.9–12.3	2.5–20	0	0.85 ± 0.10	−0.72 ± 0.10	315 ± 20	7.8[h]
CO_2	950–1090	0.9–101	—	0.18 ± 0.05	0.44 ± 0.07	—	280 ± 15	3.0[i]

[a] Temperature range.
[b] Partial pressure range of gas in feed. Total pressure is atmospheric. Diluent gas is He.
[c] Space velocity dependence (rate $\sim S^x$) over the range 0.5–4 liters (STP) g^{-1} h^{-1}.
[d] Reaction order in feed gas. Apparent reaction order for H_2O and CO_2 feeds. True reaction order for H_2O–H_2 feeds.
[e] Apparent activation energy for H_2O and CO_2 feeds. True activation energy for H_2O–H_2 feeds.
[f] Surface time yield for H_2O and CO_2 feeds. Rate for H_2O–H_2 feeds.
[g] Temperature: 1025 K. Pressure of H_2O: 12.3 kPa. Space velocity: 2.2 liters (STP) g^{-1} h^{-1}.
[h] Temperature: 1025 K. Pressure of H_2O: 12.3 kPa. Pressure of H_2: 5.4 kPa. Space velocity: 2.2 liters (STP) g^{-1} h^{-1}.
[i] Temperature: 1025 K. Pressure of CO_2: 11.1 kPa. Space velocity: 2.2 liters (STP) g^{-1} h^{-1}.

the reported rates refer only to carbon gasified to CO and CO_2. The CH_4 produced is not a product of the C–H_2O reaction, but rather of the C–H_2 reaction, as will become apparent later. The reaction was investigated under conditions where the fraction of carbon gasified to CH_4 was 20% or less.

The experimental results are summarized in Tables 3 and 4 for the uncatalyzed and platinum-catalyzed reactions, respectively. Arrhenius plots for the platinum-catalyzed gasification in H_2O–He, H_2O–H_2–He, and CO_2–He feed streams are shown in Figs. 2–4. Kinetic isotope effect results for the catalyzed C–H_2O reaction are given in Table 5. The surface time yields of catalyzed gasification of carbon by H_2O and CO_2 are compared in Table 6.

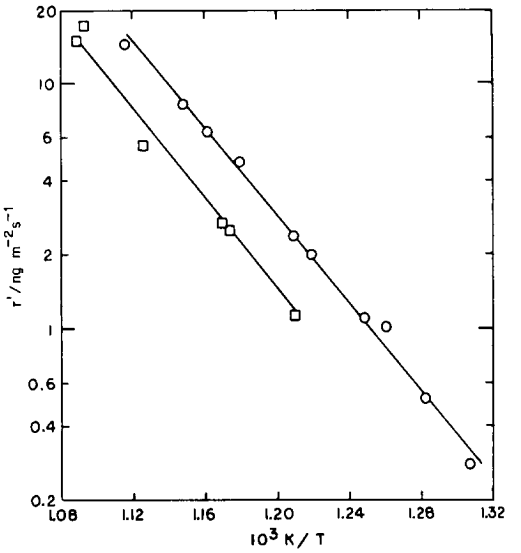

FIG. 2. Pt-Catalyzed gasification of carbon by H_2O: Arrhenius plot for the surface time yield r' of gasification of carbon. Space velocity: 2.2 liters (STP) g^{-1} h^{-1}. Pressure of H_2O: ○, 12.3 kPa; □, 2.5 kPa.

DISCUSSION

General Kinetic Considerations

The advantage of studying the catalysis of carbon reactions by a noble metal such as platinum is that platinum does not form a bulk oxide, carbide, hydroxide, or carbonate. The advantages of studying the reaction in a fixed bed reactor measuring the production rate of various gases produced

TABLE 4

Summary of Kinetic Results for the Pt-Catalyzed C–H_2O and C–CO_2 Reactions

Feed	T (K)[a]	P(kPa)[b]		x[c]	n[d]		E (kJ mol^{-1})[e]	r (ng m^{-2} s^{-1})[f]
		H_2O, CO_2	H_2		H_2O, CO_2	H_2		
H_2O	760–920	0.6–12.3	—	0.30 ± 0.05	0.44 ± 0.05	—	170 ± 10	0.14[g]
H_2O–H_2	800–970	0.7–12.3	2.0–20	0	0.53 ± 0.05	−0.5 ± 0.2	240 ± 10	2.7[h]
CO_2	800–970	0.4–101	—	0.37 ± 0.05	0.46 ± 0.05	—	170 ± 10	1.8[i]

[a] Temperature range.

[b] Partial pressure range of gas in feed. Total pressure is atmospheric. Diluent gas is He.

[c] Space velocity dependence (rate $\sim S^x$) over the range 0.5–4 liters (STP) g^{-1} h^{-1}.

[d] Reaction order in feed gas. Apparent reaction order for H_2O and CO_2 feeds. True reaction order for H_2O–H_2 feeds.

[e] Apparent activation energy for H_2O and CO_2 feeds. True activation energy for H_2O–H_2 feeds.

[f] Surface time yield for H_2O and CO_2 feeds. Rate for H_2O–H_2 feeds.

[g] Temperature: 890 K. Pressure of H_2O: 12.3 kPa. Space velocity: 2.2 liters (STP) g^{-1} h^{-1}.

[h] Temperature: 890 K. Pressure of H_2O: 12.3 kPa. Pressure of H_2: 6.2 kPa. Space velocity: 2.2 liters (STP) g^{-1} h^{-1}.

[i] Temperature: 890 K. Pressure of CO_2: 11.1 kPa. Space velocity: 2.2 liters (STP) g^{-1} h^{-1}.

TABLE 5

Rates r_{H_2O} and r_{D_2O} of the PT-Catalyzed C–H_2O and C–D_2O Reactions, Respectively[a]

T (K)	P_{H_2O}, P_{D_2O} (kPa)	P_{H_2}, P_{D_2} (kPa)	r_{H_2O} (ng m^{-2} s^{-1})	r_{D_2O} (ng m^{-2} s^{-1})	$\frac{r_{H_2O}}{r_{D_2O}}$
910	3.7	9.2	4.5	3.6	1.25
944	3.7	9.2	14.0	12.0	1.17
913	3.7	4.0	6.1	5.2	1.17
944	3.7	4.0	15.8	14.1	1.12
					1.18 ± 0.08

[a] Space velocity: 2.2 liters (STP) g^{-1} h^{-1}.

over measuring the rate gravimetrically are that product selectivities can be determined and the method is more sensitive to low reaction rates. Product selectivities can be used to investigate the secondary reactions involved. Low rates are necessary to ensure that the true kinetics are not being masked by pore diffusion effects.

Otto and Shelef (*25*) have investigated the onset of diffusion influence for the Pt-catalyzed C–H_2O reaction and concluded that it occurred at a rate of 500–5000 ng m^{-2} s^{-1} for a graphite pellet 4 mm in height and 9 mm in diameter at temperatures slightly higher and water vapor partial pressures comparable to those used in this study.

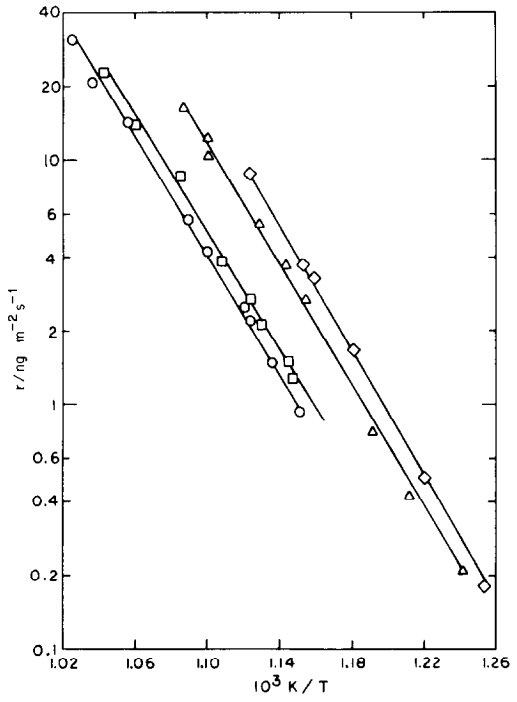

FIG. 3. Pt-Catalyzed gasification of carbon by H_2O: Arrhenius plot for the rate r of gasification of carbon. Space velocity: 2.2 liters (STP) g^{-1} h^{-1}. Pressure of H_2O: 12.3 kPa. Pressure of H_2: ◇, 1.4 kPa; △, 2.5 kPa; □, 6.2 kPa; ○, 10.1 kPa.

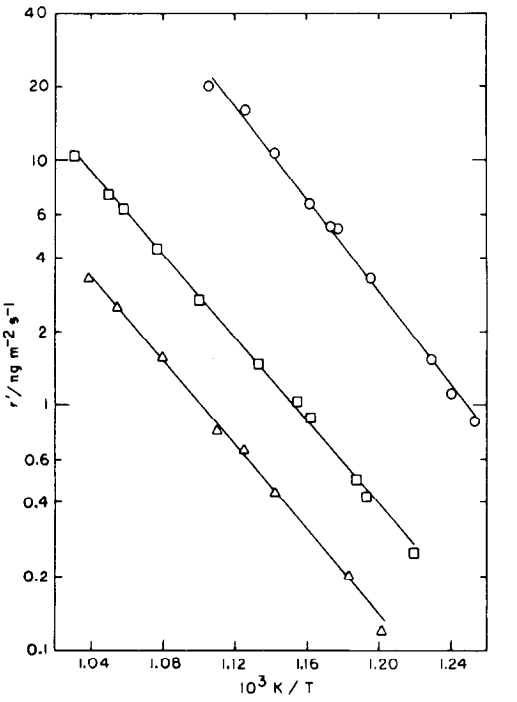

FIG. 4. Pt-Catalyzed gasification of carbon by CO_2. Arrhenius plot for the surface time yield r' of gasification of carbon. Space velocity: 2.2 liters (STP) g^{-1} h^{-1}. Pressure of CO_2: ○, atmospheric; □, 11.1 kPa; △, 1.25 kPa.

TABLE 6

Surface Time Yields r'_{H_2O} and r'_{CO_2} of the Pt-Catalyzed C–H_2O and C–CO_2 Reactions, Respectively[a]

T (K)	P_{H_2O}, P_{CO_2} (kPa)	r'_{H_2O} (ng m^{-2} s^{-1})	r'_{CO_2} (ng m^{-2} s^{-1})	$\frac{r'_{H_2O}}{r'_{CO_2}}$
893	3.3	3.5	1.14	3.1
867	11.1	2.8	0.66	4.2
893	11.1	5.3	1.5	3.6
939	11.1	10.0	2.7	3.7
				3.7 ± 0.6

[a] Space velocity: 2.2 liters (STP) g^{-1} h^{-1}.

Since the diameters of the pellets employed in this study are about 1 mm, a rate about 16 times larger (8000–80,000 ng m^{-2} s^{-1}) is necessary to obtain the same Thiele modulus (*41*). The highest rate obtained in this study, 30 ng m^{-2} s^{-1}, is thus safely within the kinetically controlled regime. It is equal to a turnover frequency of 4×10^{-5} s^{-1} with a number density of surface carbon atoms of 3.7×10^{15} cm^{-2}. Further evidence that the rates are kinetically controlled is that the platinum-catalyzed C–H_2 reaction has been shown to be kinetically controlled for similar rates at the same temperature in the same system (*6*).

However, the arguments presented above must be used with caution. For a reaction inhibited by its product, it is still possible to have internal mass transfer effects if the inhibitor term is the dominant term in the denominator and the inhibitor partial pressure changes by a large fraction over the length of a catalyst pellet (*34*). This will occur only during the gasification reactions in H_2O–He and CO_2–He feed streams and only at the entrance of the carbon bed, where the inhibitor concentration changes rapidly from zero to a finite value.

Kinetics of the Uncatalyzed Reactions

In H_2O–He mixtures (Table 3), the uncatalyzed C–H_2O reaction depends on space velocity. This can be explained by product inhibition, which results in the rate at the entrance of the bed, where the inhibitor concentration is low, being greater than the rate at the exit of the bed, where the inhibitor concentration is high. When product inhibition occurs, surface time yields are being measured—not rates—since the rate changes through the bed. The activation energies and reaction orders measured from surface time yields are not the true activation energies and reaction orders, but can rather be termed "apparent" activation energies and reaction orders. The uncatalyzed C–H_2O reaction in H_2O–He mixtures exhibits an apparent activation energy of 230 ± 20 kJ mol^{-1} and an apparent reaction order in H_2O of 0.54 ± 0.05.

If the uncatalyzed C–H_2O reaction is investigated in H_2O–H_2–He mixtures (Table 3), there is no space velocity dependence. This indicates that the reaction is inhibited by H_2, as has been widely reported in the literature (*7–11*), and that differential rates are being measured. The reaction exhibits a true activation energy of 315 ± 20 kJ mol^{-1}, a true reaction order in H_2O of 0.85 ± 0.10 and a true reaction order in H_2 of −0.72 ± 0.10 in the range of conditions investigated. The results agree with others reported in the literature (*7–11*) and can be interpreted by a Temkin rate equation for a nonuniform surface (Eq. (3)) with $n = 0.8$ or a Langmuir–Hinshelwood rate equation (Eq. (1) or (2)).

The uncatalyzed gasification of carbon by CO_2 (Table 3) exhibits a space velocity dependence of 0.18 ± 0.05, indicating that the reaction is inhibited by the product CO. The reaction exhibits an apparent activation energy of 280 ± 15 kJ mol^{-1} and an apparent reaction order in CO_2 of 0.44 ± 0.07. The results are compatible with others reported in the literature (*8, 15–17*) and can be interpreted by a Langmuir–Hinshelwood rate equation of the form of Eq. (6).

The relative surface time yields of uncatalyzed gasification by H_2O and CO_2 are between 1.5 and 3.5 over the range of conditions investigated. This compares with a relative surface time yield of 3 reported in the literature (*1*) for similar conditions.

Kinetics of the Pt-Catalyzed Reactions

Extrapolating the results to lower temperatures for the uncatalyzed reactions, we get the following relative rates of the Pt-catalyzed and uncatalyzed reactions at 890 K and a space velocity of 2.2 liters (STP) g^{-1} h^{-1}. At an H_2O partial pressure of 12.3 kPa, the surface time yield of the catalyzed $C-H_2O$ reaction is 100 times greater than that of the uncatalyzed reaction. At an H_2O partial pressure of 12.3 kPa and an H_2 partial pressure of 5.4 kPa, the differential rate of the catalyzed $C-H_2O$ reaction is 500 times greater than the uncatalyzed reaction. At a CO_2 partial pressure of 11.1 kPa, the surface time yield of the catalyzed $C-CO_2$ reaction is 100 times greater than that of the uncatalyzed reaction. These results compare to the recent observation on the same system that the catalyzed hydrogenolysis of carbon is 2000 times faster than the uncatalyzed hydrogenolysis at 890 K and atmospheric hydrogen pressure (*6*). Extrapolating the results for hydrogenolysis to lower pressure indicates that at 890 K and a H_2 partial pressure of 12 kPa, the catalyzed hydrogenolysis is 40,000 times faster than the uncatalyzed hydrogenolysis. The addition of 1.5% platinum to Spheron 6 has been found to increase the rate of carbon oxidation by a factor of 20 at 663 K and an O_2 partial pressure of 12 kPa (*33*).

The Pt-catalyzed gasification of carbon in H_2O-He mixtures (Table 4) exhibits a space velocity dependence of 0.30 ± 0.05, indicating that product inhibition is occurring. The reaction has an apparent activation energy of 170 ± 10 kJ mol^{-1} (Fig. 2) and an apparent reaction order in H_2O of 0.44 ± 0.05.

The Pt-catalyzed gasification of carbon by H_2O-H_2-He mixtures (Table 4) exhibits no space velocity dependence, so that differential rates are being measured. The reaction exhibits a true activation energy of 240 ± 10 kJ mol^{-1} (Fig. 3), a true reaction order in H_2O of 0.53 ± 0.05 and a true reaction order in H_2 of -0.5 ± 0.2. These results indicate that the Pt-catalyzed $C-H_2O$ reaction is inhibited by H_2, a result which has been overlooked in the past.

In two previous kinetic studies of the Pt-catalyzed $C-H_2O$ reaction (*24, 25*), reaction orders and space velocity dependences were not determined. Thus the inhibition of the reaction by H_2 went unnoticed. Indeed, Otto and Shelef (*25*) report that the conversion of H_2O was kept low so that hydrogen inhibition would not be a problem. In this study it appears that hydrogen inhibition is a factor for H_2 pressures at least as low as 0.1 kPa and probably much lower.

Rewick *et al.* (*24*) studied the Pt-catalyzed $C-H_2O$ reaction in a flow-through gravimetric bed reactor using an H_2O-He feed stream. An activation energy of 175 ± 15 kJ mol^{-1} can be calculated from their graphical results. This compares very well with the apparent activation energy of 170 ± 10 kJ mol^{-1} determined in this investigation for an H_2O-He feed stream.

Otto and Shelef (*25*) studied the reaction in a recirculating gravimetric bed reactor and report that the rates were measured after an amount of time long enough that a constant rate was achieved. The result of this procedure was probably that a partial pressure of H_2 was produced by the reaction before rate measurements were made which then remained fairly constant over the course of the time that rate measurements were recorded for the activation energy. Thus the activation energy reported represents that for constant H_2O and H_2 partial pressures. A later paper (*26*) indicates that this is the case. Their reported activation energy of 250 kJ mol^{-1} agrees with the true activation energy of 240 ± 10 kJ mol^{-1} obtained in this study for H_2O-H_2-He feeds.

Thus the difference in activation energies reported by Otto and Shelef and calculated from the data of Rewick *et al.* is readily explained by the different experimental arrangements. The agreement between the activation energies determined in this study and that of the previous studies is excellent,

despite the fact that different carbons were used in each investigation. Recently, excellent agreement in activation energies has also been reported in different studies for the Pt-catalyzed hydrogenolysis of carbon (*6*).

Within experimental error, the differential rate, r, of the Pt-catalyzed C–H_2O reaction can be expressed by

$$r = k[(H_2O)/(H_2)]^n, \qquad (8)$$

where k is the rate constant for the reaction and $n = 0.5$. If it is assumed that there is no backmixing of gases in the reactor (plug flow), this equation can be integrated through the carbon bed to obtain the surface time yield, r', for H_2O–He feeds. When there is no hydrogen in the feed stream for the catalyzed reaction, the CO_2/CO ratio in the product gas is always observed to be greater than 5. Assuming that CO_2 and H_2 are the only products, the reaction can be written

$$C + 2H_2O = CO_2 + 2H_2.$$

Equation (8) may be integrated through the bed to give the expected surface time yield, r':

$$r' = [k(1 + n)]^{1/(1+n)}\left[\frac{SMCP_{H_2O}}{2\alpha P}\right]^{n/(1+n)}, \qquad (9)$$

where k/ng m^{-2} s^{-1} is the rate constant, P_{H_2O}/kPa is the H_2O partial pressure, P/kPa is the total pressure, S/liters (STP) g^{-1} h^{-1} is the space velocity, α/m^2 g^{-1} is the initial BET surface area of carbon, $M = 12$ g mol^{-1} is the atomic weight of carbon and $C = 1.240$ ng mol h g^{-1} liters $(STP)^{-1}$ s^{-1} is a conversion constant. For $n = 0.5$

$$r' \sim k^{0.67}P_{H_2O}^{0.33}S^{0.33}.$$

Since

$$k = Ae^{-E/RT}$$

the expected apparent activation energy, E', is

$$E' = 0.67E.$$

For the results obtained in this study with H_2O–He feed streams, the catalyzed C–H_2O reaction exhibits a space velocity dependence of 0.30 ± 0.05, an apparent reaction order in H_2O of 0.44 ± 0.05 and an apparent activation energy of 0.71 ± 0.07 E. The experimental values compare quite well with the expected values calculated from the differential rate equation. Differences may be attributed either to a small amount of backmixing in the reactor, to the differential rate equation (Eq. (8)) not holding at the bed entrance where the hydrogen pressure is very low, or to internal mass transfer effects influencing the kinetics at the bed entrance as previously discussed.

The Pt-catalyzed gasification of carbon in CO_2–He feed mixtures (Table 4) exhibits a space velocity dependence of 0.37 ± 0.05, indicating that the reaction is inhibited by the product CO. As with the C–H_2O reaction, the uncatalyzed C–CO_2 reaction has long been known to be inhibited by its product, but this inhibition has generally been ignored for the catalyzed reaction. The apparent activation energy is 170 ± 10 kJ mol^{-1} (Fig. 4) and the apparent reaction order in CO_2 is 0.46 ± 0.05.

It was not possible to study the Pt-catalyzed C–CO_2 reaction differentially using CO_2–CO–He feed mixtures since rates were determined by measuring the amount of carbon monoxide produced.

The surface time yields of the Pt-catalyzed C–H_2O and C–CO_2 reactions exhibit similar space velocity dependences, similar reaction orders in the reactant gas, and similar activation energies (Table 4). This indicates that the rate of the Pt-catalyzed C–CO_2 reaction can be expressed by a differential rate equation of the form used for the C–H_2O reaction:

$$r = k[(P_{CO_2})/(P_{CO})]^n, \qquad (10)$$

where k is the rate constant and $n = 0.5$. The true activation energy for the reaction is 240 ± 30 kJ mol^{-1}.

Product Selectivities of the Uncatalyzed and Pt-Catalyzed C–H_2O Reactions

There are four possible products of the C–H_2O reaction: CO, CO_2, CH_4, and H_2. The selectivity of the reaction to these products will depend on the relative rates of reactions (I)–(V). The selectivities of carbon gasification to CO, CO_2, and CH_4 are defined to be the fraction of carbon gasified to each of these products.

In addition to catalyzing the C–H_2O and C–CO_2 reactions, platinum will also catalyze the forward (*42*) and reverse (*43*) water–gas shift, methanation (*44*), and hydrogenolysis of carbon (*6*). Carbon, by contrast, is a poor catalyst for water–gas shift (*8*) and methanation. It is reasonable to expect that for Pt/C, all of the reactions are occurring on the platinum or at the platinum–carbon interface.

The ratio of the forward rate, $\vec{r}_i$, to the reverse rate, $\overleftarrow{r}_i$, of reaction (i) at the reactor exit is given by

$$\frac{\vec{r}_i}{\overleftarrow{r}_i} = \frac{K_i}{K_i^*} = e^{Ai/\bar{\chi}_i RT}, \qquad (11)$$

where A_i is the affinity of the reaction, $\bar{\chi}_i$ is the average stoichiometric number of the reaction, K_i is the equilibrium constant of the reaction, and K_i^* is the value of the equilibrium constant away from equilibrium calculated from the partial pressures of the gases at the reactor exit (*45*). The overall rate of reaction (i), r_i, is given by

$$r_i = \vec{r}_i - \overleftarrow{r}_i.$$

If $K_i = K_i^*$, the reaction is equilibrated at the reactor exit ($r_i = 0$); if $K_i > K_i^*$, $r_i > 0$; if $K_i < K_i^*$, $r_i < 0$.

The products of the uncatalyzed C–H_2O reaction were predominantly CO and H_2. No CH_4 was observed. The selectivity of carbon gasification to CO_2 was less than 20% for H_2O–He feeds and in the range of 15 to 40% for H_2O–H_2–He feeds. Selectivity to CO_2 was favored by low space velocities, indicating that it is not produced directly, but rather through the secondary water–gas shift reaction, as has been widely reported (*8*). Observed values of K_i/K_i^* for reactions (I), (II), and (V) are reported in Table 7. Of particular note is that the water–gas shift reaction is not equilibrated, indicating that the steps

$$\ldots C\text{–}C^* + H_2O = \ldots C\text{–}C\text{–}O + H_2$$

and

$$\ldots C\text{–}C\text{–}O + CO = \ldots C\text{–}C^* + CO_2$$

cannot both be equilibrated.

TABLE 7

K_i/K_i^* for Reactions (1)–(5) for the Uncatalyzed C–H_2O Reaction

Reaction[a]	K_i/K_i^*[b]	
	H_2O Feed[c]	H_2O–H_2 Feed[d]
1	>20,000	>10,000
2	>100	10–25
3	*e*	*e*
4	*e*	(≪1)[f]
5	>50	>500

[a] Reactions defined in Introduction.

[b] Defined by Eq. (11).

[c] Temperatue: 940–1070 K. Partial pressure of H_2O: 0.8–12.3 kPa. Total pressure: atmospheric. Space velocity: 0.5–4 liters (STP) g^{-1} h^{-1}.

[d] Temperature: 980–1100 K. Partial pressure of H_2O: 0.9–12.3 kPa. Partial pressure of H_2: 2.5–20 kPa. Total pressure: atmospheric. Space velocity: 0.5–4 liters (STP) g^{-1} h^{-1}.

[e] Not determined. CH_4 undetected and predicted to be undetectable from K_i.

[f] CH_4 undetected but predicted to be detectable from K_i.

The products of the Pt-catalyzed C–H_2O reaction in H_2O–He feed streams were primarily CO_2 and H_2. No CH_4 was observed. The selectivity of carbon gasification to CO_2 ranged from 80 to 95%. In H_2O–H_2–He feeds, production of CO, CO_2, and CH_4 was observed. The selectivity of carbon gasification to CO_2 (25 to 80%) increased with decreasing space velocity, indicating that, as with the uncatalyzed reaction, CO_2 is produced from CO through water–gas shift. The observed values of K_i/K_i^* are

TABLE 8

K_i/K_i^* for Reactions (1)–(5) for the Pt-Catalyzed C–H_2O Reaction

Reaction[a]	K_i/K_i^*[b]	
	H_2O Feed[c]	H_2O–H_2 Feed[d]
1	>2000	>1000
2	1.1–2.0	1.2–3.3
3	*e*	<0.01
4	*e*	3–5
5	>2000	>1000

[a] Reactions defined in Introduction.

[b] Defined by Eq. (11).

[c] Temperature: 760–920 K. Pressure of H_2O: 0.6–12.3 kPa. Total pressure: atmospheric. Space velocity: 0.5–4 liters (STP) g^{-1} h^{-1}.

[d] Temperature: 800–970 K. Pressure of H_2O: 0.7–12.3 kPa. Pressure of H_2: 2.0–20 kPa. Total pressure: atmospheric. Space velocity: 2.2 liters (STP) g^{-1} h^{-1}.

[e] Not determined. CH_4 undetected and predicted to be undetectable from K_i.

given in Table 8. Of particular note is that the methanation reaction is far to the right of equilibrium, indicating that methane is produced only through hydrogenolysis of carbon. It is not a product of the C–H_2O reaction. The water–gas shift and hydrogenolysis reactions are only slightly to the left of equilibrium. Only three of the five reactions are linearly independent. It is apparent from Table 8 that those which should be considered are

$$C + H_2O \rightarrow CO + H_2,$$
$$CO + H_2O \rightleftharpoons CO_2 + H_2,$$
$$C + 2H_2 \rightleftharpoons CH_4.$$

Rewick *et al.* (*24*) observed CO and H_2 as the only products of the Pt-catalyzed C–H_2O reaction for H_2O–He feeds. This is in complete disagreement with the selectivities to CO_2 greater than 80% observed in this study under similar conditions. Tamai *et al.* (*22*) calculated theoretical CO_2/CO product ratios based on equilibrium of reactions (I) and (II). This implies that reaction (V) is equilibrated. The experimental CO_2/CO ratio was always much less than predicted. As noted in this study (Table 8) reaction (V) is always far from equilibrium. The CO_2/CO ratio can be predicted by assuming the water–gas shift reaction (reaction (II)) is equilibrated.

Proposed Mechanisms for the Pt-Catalyzed C–H_2O and C–CO_2 Reactions

The results for the uncatalyzed C–H_2O and C–CO_2 reactions support the previously proposed mechanisms for these reactions (*1*) described in the Introduction.

The Pt-catalyzed C–H_2O reaction is proposed to occur through the following series of steps:

$$\ldots C\text{–}C\text{–}C + Pt^* \underset{k_{-1}}{\overset{k_1}{\rightleftharpoons}} \ldots C\text{–}C + Pt^*\text{–}C,$$

$$Pt^* + H_2O \overset{K_2}{\rightleftharpoons} Pt^*\text{–}O + H_2,$$

$$Pt^*\text{–}C + Pt^*\text{–}O \xrightarrow{k_3} 2\,Pt^* + CO.$$

CO_2 is then produced through the step

$$Pt^*\text{–}O + CO \underset{k_3}{\overset{k_{-3}}{\rightleftharpoons}} Pt^* + CO_2.$$

completing the water–gas shift. Methane is produced through a series of steps summarized by

$$Pt^*\text{–}C + 2H_2 \rightleftharpoons Pt^* + CH_4.$$

Similarly, the Pt-catalyzed C–CO_2 reaction is proposed to occur through the steps:

$$\ldots C\text{–}C\text{–}C + Pt^* \underset{k_{-1}}{\overset{k_1}{\rightleftharpoons}} \ldots C\text{–}C + Pt^*\text{–}C,$$

$$Pt^* + CO_2 \overset{K_2}{\rightleftharpoons} Pt^*\text{–}O + CO,$$

$$Pt^*\text{–}C + Pt^*O \xrightarrow{k_4} 2\,Pt^* + CO.$$

The first step of both reactions is the reversible formation of carbidic carbon on platinum Pt^*–C from bulk carbon C–C–C. The second step is equilibrated. Thus the concentration of adsorbed oxygen on the Pt is a function of the H_2O/H_2 partial pressure ratio for the C–H_2O reaction and the CO_2/CO partial pressure ratio for the C–CO_2 reaction. The final step, the production of

CO by reaction of adsorbed carbon with adsorbed oxygen on the Pt surface, is irreversible under the conditions at which the reactions were studied. The evidence that the carbon–carbon bonds are broken directly by the Pt without the participation of adsorbed oxygen on the Pt is that this step has been shown to be rate-determining for the Pt-catalyzed C–H_2 reaction (*6*), which is nearly equilibrated ($K_4/K_4^* \cong 1$) during the C–H_2O reaction.

At the high temperatures and H_2O/H_2 (or CO_2/CO) partial pressure ratios used in this study, the fraction of Pt covered with adsorbed oxygen is expected to be small (*46*). The fraction covered with adsorbed carbon is also assumed to be small. The use of uniform surface kinetics is justified for small surface coverages and the proposed mechanisms yield the rate equations:

H_2O:

$$r = \frac{k_1 k_4 K_2[(H_2O)/(H_2)]}{k_4 K_2[(H_2O)/(H_2)] + k_{-1}}, \quad (12)$$

CO_2:

$$r = \frac{k_1 k_4 K_3[(CO_2)/(CO)]}{k_4 K_3[(CO_2)/(CO)] + k_{-1}}. \quad (13)$$

If the first step were rate determining, the rate of the Pt-catalyzed C–H_2O reaction would reduce to

$$r = k_1.$$

The kinetic isotope effect, r_{H_2O}/r_{D_2O}, would be

$$r_{H_2O}/r_{D_2O} = 1.00$$

since the first step does not involve participation of hydrogen atoms. If the third step were rate determining, the rate would reduce to

$$r = (k_1/k_{-1})k_4 K_2[(H_2O)/(H_2)].$$

The kinetic isotope would be determined solely by differences in K_2 for H_2O and D_2O, since hydrogen atoms, in H_2O or H_2, participate only in the second step. The expected kinetic isotope effect would be

$$\frac{r_{H_2O}}{r_{D_2O}} = K_{ex},$$

where K_{ex} is the equilibrium constant for the isotope exchange reaction

$$D_2O + H_2 = H_2O + D_2.$$

K_{ex} is readily calculated from thermodynamic data for hydrogen (*47, 48*), deuterium (*48, 49*), water (*50*), and deuterated water (*50*) to be 1.64 at 910 K and 1.58 at 944 K.

Experimentally, the reaction has been found to be 0.5 order in the H_2O/H_2 partial pressure ratio and to exhibit a kinetic isotope effect of 1.18 ± 0.08 (Table 7) from 910 to 944 K. These results are consistent with a rate expression of the form of Eq. (12) and imply that neither the first nor third step may be considered to be rate determining. The kinetic isotope effect is thermodynamic in origin. It does not result from a difference in the rates of breakage of O–H and O–D bonds, but rather from a difference in the concentration of adsorbed oxygen on the platinum in H_2O/H_2 and D_2O/D_2 atmospheres.

The proposed mechanisms indicate that the rates of the Pt-catalyzed C–H_2O and C–CO_2 reactions should be similar. The surface time yield has been found to be 3.7 ± 0.6 times faster for the C–H_2O reaction than for the C–CO_2 reaction (Table 8). The proposed mechanisms also indicate that the two reactions should exhibit similar reaction orders, as has been observed. If the first step were rate determining, both reactions would be expected to have the same activation energy. If the third step were rate determining, the difference in activation energies would be given by

$$E_{CO_2} - E_{H_2O} = -\Delta H_W,$$

where ΔH_W is the heat of reaction for the water–gas shift reaction (−36 kJ mol^{-1} at 900 K). Since neither step is rate determining the activation energy for the Pt-catalyzed C–CO_2 reaction is expected to be

between 0 and 36 kJ mol^{-1} greater than that for the $C-H_2O$ reaction. This is consistent with the identical activation energies observed within an experimental error of about 25 kJ mol^{-1}.

In analyzing the kinetics of the catalyzed $C-H_2O$ reaction, the simultaneous gasification of carbon by H_2 to CH_4 must be considered. It has been found that the amount of methane produced during the $C-H_2O$ reaction is limited by equilibration of the hydrogenolysis of carbon, but may greatly exceed the amount predicted by methanation equilibrium. This suggests that the thermal efficiency of a catalytic coal gasification process may be improved by selection of a catalyst which accelerates the $C-H_2$ reaction as well as the $C-H_2O$ reaction.

ACKNOWLEDGMENT

This work was supported by the Department of Energy AS03-76SF10502.

REFERENCES

1. Walker, P. L., Rusinko, F., and Austin, L. G., *in* "Advances in Catalysis and Related Subjects," Vol. 11, p. 133. Academic Press, New York/London, 1959.
2. Lewis, J. B., *in* "Modern Aspects of Graphite Technology" (L. C. F. Blackman, Ed.), p. 129. Academic Press, New York/London, 1970.
3. McKee, D. W., *Chem. Phys. Carbon* **16,** 1 (1981).
4. Wen, W. Y., *Catal. Rev. Sci. Eng.* **22,** 1 (1980).
5. Walker, P. L., Jr., Shelef, M., and Anderson, R. A., *Chem. Phys. Carbon* **4,** 287 (1968).
6. Holstein, W. L., and Boudart, M., *J. Catal.* **72,** 328 (1981).
7. Johnstone, H. F., Chen. C. Y., and Scott, D. S., *Ind. Eng. Chem.* **44,** 1564 (1952).
8. Gadsby, J., Hinshelwood, C. N., and Sykes, K. W., *Proc. R. Soc. A* **187,** 129 (1946).
9. Long, F. J., and Sykes, K. W., *Proc. R. Soc. A* **193,** 377 (1948).
10. Giberson, R. C., and Walker, J. P., *Carbon* **3,** 521 (1966).
11. Cherednik, E. M., Apel'baum, L. O., and Temkin, M. I., *Dokl. Akad. Nauk. SSSR* **174,** 891 (1966).
12. Blyholder, G., and Eyring, H., *J. Phys. Chem.* **63,** 693 (1959).
13. Blakely, J. P., and Overholser, L. G., *Carbon* **3,** 269 (1965).
14. Montet, G. C., and Myers, G. E., *Carbon* **6,** 627 (1968).
15. Strange, J. F., and Walker, P. L., Jr., *Carbon* **14,** 345 (1976).
16. Golovina, E. S., *Carbon* **18,** 197 (1980).
17. Rief, A. E., *J. Phys. Chem.* **56,** 785 (1952).
18. Ergun, S., and Mentser, M., *Chem. Phys. Carbon* **1,** 203 (1966).
19. Temkin, M. I., Cherednik, E. M., and Apel'baum, L. O., *Kinet. Katal.* **9,** 95 (1966).
20. Turkdogan, E. T., and Vinters, J. V., *Carbon* **10,** 97 (1972).
21. McKee, D. W., *Fuel* **59,** 308 (1980).
22. Tamai, Y., Watanabe, H., and Tomita, A., *Carbon* **15,** 103 (1977).
23. McKee, D. W., *Carbon* **12,** 453 (1974).
24. Rewick, R. T., Wentrcek, P. R., and Wise, H., *Fuel* **53,** 274 (1974).
25. Otto, K., and Shelef, M., *Carbon* **15,** 317 (1977).
26. Otto, K., Bartosiewicz, L., and Shelef, M., *Carbon* **17,** 351 (1971).
27. Long, F. J., and Sykes, K. W., *J. Chim. Phys.* **47,** 361 (1950).
28. Grabke, H. J., *Carbon* **10,** 587 (1972).
29. McKee, D. W., and Chatterji, D., *Carbon* **16,** 53 (1978).
30. McKee, D. W., and Chatterji, D., *Carbon* **13,** 381 (1975).
31. McKee, D. W., *Fuel* **59,** 308 (1980).
32. Franke, F. H., and Meraikib, M., *Carbon* **8,** 423 (1970).
33. Marsh, H., and Rand, B., *Carbon* **9,** 63 (1971).
34. Austin, L. G., and Walker, P. L., *AIChE J.* **9,** 303 (1963).
35. Tashiro, J., Takakuwa, I., and Yokoyama, S., *Fuel* **55,** 250 (1976).
36. Robell, A. J., Ballou, E. V., and Boudart, M., *J. Phys. Chem.* **68,** 2748 (1964).
37. Amirnazmi, A., Benson, J. E., and Boudart, M., *J. Catal.* **30,** 55 (1973).
38. Lange, N. A. (Ed.), "Handbook of Chemistry." McGraw-Hill, New York, 1961.
39. Kazavchinskii, Y. Z., "Heavy Water." Israeli Program for Scientific Translations, Ltd., Jerusalem, 1971.
40. Benson, J. E., and Boudart, M., *J. Catal.* **4,** 704 (1965).
41. Satterfield, C. N., and Sherwood, T. K., "The Role of Diffusion in Catalysis." Addison-Wesley, Reading, Mass., 1963.
42. Grenoble, D. C., Estadt, M. M., and Ollis, D. F., *J. Catal.* **67,** 90 (1981).
43. Masuda, M., and Miyahara, K., *Bull. Chem. Soc. Japan* **47,** 1058 (1974).
44. Vannice, A., *J. Catal.* **40,** 129 (1975).
45. Boudart, M., *J. Phys. Chem.* **80,** 2869 (1976).
46. Gonzalez, O. D., and Parravano, G., *J. Amer. Chem. Soc.* **78,** 4533 (1956).

47. Wagman, D. D., Kilpatrick, J. E., Taylor, W. J., Pitzer, K. S., and Rossini, F. D., *J. Res. Natl. Bur. Stand.* **34,** 143 (1945).
48. Landolt-Bornstein, "Zählenwerte und Funktionen II. Band Eigenschaften der Materie in Ihren Aggregratzustanden. 4. Teil. Kalorische Zustandgrössen" (K. Schafer and E. Lax, Eds.). Springer Verlag, Berlin, 1961.
49. Wooley, H. W., Scott, R. B., and Brickwedde, F. G., *J. Res. Natl. Bur. Stand.* **41,** 399 (1948).
50. Friedman, A. S., and Haar, L., *J. Chem. Phys.* **22,** 2051 (1954).